NIH Public Access
Author Manuscript
J Magn Reson Imaging. Author manuscript; available in PMC 2011 November 1.

Published in final edited form as:
J Magn Reson Imaging. 2010 November ; 32(5): 1124–1131. doi:10.1002/jmri.22362.

Association Between Serial Dynamic Contrast-Enhanced MRI and Dynamic ^{18}F-FDG PET Measures in Patients undergoing Neoadjuvant Chemotherapy for Locally Advanced Breast Cancer

Savannah C. Partridge, PhD[1], **Risa K. Vanantwerp**[2], **Robert K. Doot, PhD**[3], **Xiaoyu Chai, MS**[4], **Brenda F. Kurland, PhD**[4], **Peter R. Eby, MD**[1], **Jennifer M. Specht, MD**[5], **Lisa K. Dunnwald, MPH**[3], **Erin K. Schubert, BS**[3], **Constance D. Lehman, MD, PhD**[1], and **David A. Mankoff, MD, PhD**[1,3]

[1] Department of Radiology, University of Washington, Seattle, WA

[2] Department of Bioengineering, University of Washington, Seattle, WA

[3] Department of Nuclear Medicine, University of Washington, Seattle, WA

[4] Division of Clinical Statistics, Fred Hutchinson Cancer Research Center, Seattle, WA

[5] Department of Medicine, University of Washington, Seattle, WA

Abstract

Purpose—To investigate the relationship between changes in vascularity and metabolic activity measured by dynamic contrast-enhanced MRI (DCE-MRI) and dynamic ^{18}F-FDG-positron emission tomography (PET) in breast tumors undergoing neoadjuvant chemotherapy.

Materials and Methods—PET and MRI examinations were performed in 14 patients with locally advanced breast cancer (LABC) before and after chemotherapy. Dynamic ^{18}F-FDG PET measures included ^{18}F-FDG transport rate constant from blood to tissue (K_1) and metabolism flux constant (Ki). DCE-MRI measures included initial peak enhancement (PE), signal enhancement ratio (SER), and tumor volume. Spearman rank-order correlations were assessed between changes in PET and MRI parameters, and measures were compared between patients with and without pathologic complete response (pCR) by Mann-Whitney U test.

Results—Changes in glucose delivery (PET K_1) were closely correlated with changes in tumor vascularity as reflected by DCE-MRI SER (ρ=0.83, $p<0.001$). Metabolic changes in PET Ki showed moderate correlations with vascularity changes as reflected by SER (ρ=0.71) and PE (ρ=0.76), and correlated closely with MRI tumor volume (ρ=0.79, $p<0.001$). Decreases in K_1, Ki, SER, and PE were greater for patients with pCR compared to those with residual disease ($p<0.05$).

Conclusion—Dynamic ^{18}F-FDG PET and DCE-MRI tumor measures of tumor metabolism, vascularity, and volume were well correlated for assessing LABC response to neoadjuvant chemotherapy and significantly discriminated pathologic complete responders. Further work is necessary to assess the value of combined PET and MRI for evaluating tumor pharmacodynamics in response to novel therapy.

Address Correspondence and Reprint Requests To: Savannah Partridge, PhD, Research Assistant Professor of Radiology, University of Washington School of Medicine, Seattle Cancer Care Alliance, 825 Eastlake Ave. E., G3-200, Seattle, WA 98109-1023, Phone: (206) 288-1306, Fax: (206) 288-6556, scp3@u.washington.edu.

NIH-PA Author Manuscript
NIH-PA Author Manuscript
NIH-PA Author Manuscript

NIH-PA Author Manuscript

NIH-PA Author Manuscript

NIH-PA Author Manuscript

Keywords

dynamic ^{18}F-FDG positron emission tomography (PET); dynamic contrast-enhanced MRI (DCE-MRI); pathologic response; treatment; locally advanced breast cancer

INTRODUCTION

Neoadjuvant chemotherapy followed by surgical resection is commonly used for treatment of locally advanced breast cancer (LABC) and offers advantages over traditional adjuvant approaches. Accurate methods to monitor response in the tumor and predict outcome early in the course of treatment would improve our ability to individualize therapies. Dynamic contrast-enhanced MRI and dynamic ^{18}F-fluorodeoxyglucose (FDG) PET are two imaging modalities that can provide valuable insight to assess treatment efficacy. PET measures of blood flow and metabolism using ^{15}O-water and ^{18}F-FDG, both pre- and mid-therapy, predict response to chemotherapy in patients with LABC (1–6). Similarly, DCE-MRI measures of tumor vascularity and functional volume before and during treatment are predictive of response and recurrence-free survival (7–10). The combination of blood flow and metabolism measured by ^{15}O-water and ^{18}F-FDG offers unique insights into in vivo breast cancer biology and predicts response to treatment (1,11). Since ^{15}O-water PET poses a logistical challenge due to the short half life of ^{15}O, studies have used a combination of methods in conjunction with FDG PET to measure tumor perfusion and vascularity, including dynamic contrast-enhanced CT (12), DCE-MRI (13), and dynamic FDG PET (1,14), with somewhat similar results. The combination of DCE-MRI and ^{18}F-FDG PET, two imaging modalities commonly used in the clinical management of breast cancer, provides a practical and attractive combination that may predict treatment response better than either modality alone.

A limited number of studies have investigated and compared FDG PET and DCE MRI for assessing breast cancer in the same patients. For breast tumor characterization prior to treatment, some reports suggested that the relationship between measures of tumor metabolism by PET and perfusion by DCE-MRI was predictive of response (13,15). In a prior study, tumor DCE-MRI kinetics in untreated breast cancers correlated well with blood flow measures by ^{15}O-water PET, but did not correlate with ^{18}F-FDG PET metabolic rate (16). The relationship between FDG PET and DCE-MRI for predicting breast cancer treatment response has been investigated previously (17,18): Semple et al. showed that pre-therapy DCE-MRI vascular parameters predicted early change in PET metabolic measures (18), and Chen et al. found that MRI measures of tumor size and PET measures of SUV were complementary for predicting pathological response (17). However, neither study assessed the relationship between the changes in DCE-MRI kinetics and PET metabolic measures with treatment.

Our overall goal is to better direct the use of PET and MRI in breast cancer response monitoring. The two imaging techniques are functionally very different and the extent of their agreement or discordance for monitoring functional changes in tumors is not well understood. Therefore, the primary purpose of this study was to evaluate the association between changes in tumor volume, vascularity and metabolic activity measured by DCE-MRI and dynamic ^{18}F-FDG-PET in patients undergoing neoadjuvant chemotherapy. We further compared changes measured by PET and MRI in patients with and without pathologic complete response.

NIH-PA Author Manuscript

NIH-PA Author Manuscript

NIH-PA Author Manuscript

MATERIALS AND METHODS

Patient Selection

This study was approved by our institutional review board and was compliant with the Health Insurance Portability and Accountability Act. Eligible patients were those who presented at the University of Washington Breast Cancer Specialty Clinic with locally-advanced breast cancer (LABC) and participated in a prospective trial of PET to evaluate response to neoadjuvant therapy. Inclusion criteria for the study were breast tumors greater than 5 cm, or a tumor of any size with skin or chest wall involvement, involving a substantial portion of a small breast, or with advanced axillary disease. All patients signed prospective informed consent for review of their imaging results and medical records. Retrospective review was performed on medical records of patients enrolled in the PET trial who underwent neoadjuvant chemotherapy between February 2004 and July 2007. Patients in the study underwent a neoadjuvant regimen of weekly metronomic doxorubicin-based chemotherapy with daily oral cyclophosphamide for 12 weeks followed by 12 weeks of paclitaxel (plus trastuzumab in patients with HER-2/*neu*-overexpressing breast cancer). Patients included in this study had two or more breast MRI examinations and two or more PET studies during treatment, with corresponding PET and MRI scans less than four weeks apart. After treatment, all patients underwent surgery, either mastectomy or lumpectomy.

MRI Acquisition

MRI examinations were performed on a GE LX 1.5T scanner (General Electric Medical Systems, Waukesha, WI) using a dedicated bilateral breast coil (February 2004 through September 2005: MRI Devices7-Channel Biopsy Breast Array, from October 2005 on: GE 8-Channel Phased Array Breast Coil). The clinical breast DCE-MRI protocol at our institution was optimized for accurate detection and staging, providing images with high spatial resolution, fat suppression, and bilateral coverage. The DCE-MRI sequence for all examinations included one pre- and at least 3 post-contrast T1-weighted 3D fast spoiled gradient echo (FSPGR) acquisitions, acquired with the Volume Imaging for Breast Assessment (VIBRANT) parallel imaging technique (GE). From February 2004 through June 2006, the DCE-MRI sequence incorporated a 90 second acquisition (TR=6.7ms, TE=4.2ms, flip angle=10°), and at least three post-contrast acquisitions centered at 90, 180, and 270 seconds after contrast injection. The acquisition matrix was 350 × 350 and spatial resolution was 1.0 × 1.0 mm in-plane with 2.2 mm slice thickness. After June 2006, the DCE-MRI sequence was changed to improve spatial resolution and incorporated a 3 minute acquisition (TR=5.6ms, TE=2.6ms, flip angle=10°) with post-contrast acquisitions centered at 90, 270, and 450 seconds after contrast injection. The acquisition matrix was 420 × 420 and spatial resolution was 0.85 × 0.85 × 1.6 mm. The contrast agent administered was 0.1 mmol/kg body-weight Gd-DTPA (Omniscan, GE Healthcare). Twelve of the 14 patients underwent the same DCE-MRI protocol (either the 90 second or 3 minute) for both MRI examinations, while two patients underwent the 90 second protocol for their baseline scan and the 3 minute protocol for their follow-up scan due to the timing of their treatment spanning the change in clinical breast MRI protocol.

MR Image Analysis

DCE-MRI images were analyzed using semi-automated software written in-house in Java language and ImageJ (NIH, public domain). Semiquantitative DCE-MRI kinetic parameters were calculated based on the signal enhancement ratio method, as previously described (8,16,19). Contrast kinetics were characterized by two parameters 1) the initial peak enhancement (PE) and 2) the delayed signal enhancement ratio (SER). PE reflects the degree of signal enhancement in the tumor at 90 seconds after contrast delivery, calculated by

NIH-PA Author Manuscript

NIH-PA Author Manuscript

NIH-PA Author Manuscript

$$PE = \frac{S_1 - S_0}{S_0} \times 100\% \quad [1]$$

Where S_0 is the MRI signal intensity prior to contrast and S_1 is the MRI signal intensity 90 seconds after contrast delivery. SER reflects the rate of contrast washout in the tumor between 90 and 270 seconds after contrast delivery, calculated by

$$SER = \frac{S_1 - S_0}{S_2 - S_0} \quad [2]$$

where S_2 is the MRI signal intensity at 270 seconds after contrast delivery. PE and SER were calculated on a voxel-by-voxel basis within the tumor, with SER calculated only for voxels with at least 50% PE. Functional tumor volume was calculated by summing all voxels with PE ≥ 50%, as previously described (10,19). The software automatically identified hot-spot regions of peak PE and peak SER that were defined as eight contiguous voxels producing the highest mean PE and SER value, respectively. In the case of very low signal enhancement where PE was less than 50% (such as in complete responders), peak PE and peak SER were calculated manually from an ROI drawn free-hand in the area of prior enhancement.

PET Acquisition

Each patient in the study underwent serial dynamic ^{18}F-FDG PET examination according to the University of Washington Human Subjects Committee guidelines. The data from some of these examinations have been previously published along with a description of the experimental protocol (3,4,14). In summary, PET images were obtained on an Advance Tomograph (GE Medical Systems, Waukesha, WI) with 35 transaxial planes, 4.25 mm thick. Imaging was performed using a two-minute infusion of 260-407 MBq (7–11 mCi) of ^{18}F-FDG. Glucose concentrations were checked immediately prior to administration of ^{18}F FDG (range = 60–170 mg/dL; mean = 93 mg/dL). Dynamic images were obtained for 60 min. The dynamic imaging sequence was 4 × 20 s, 4 × 40 s, 4 × 1 min, 4 × 3 min and 8 × 5 min.

PET Image Analysis

Tumor regions of interest (ROI) were drawn as 1.5 cm diameter circles on the ^{18}F-FDG images around the area of maximum tumor activity over three contiguous planes chosen to be the most biologically aggressive portion of the tumor as previously described (14). The blood clearance curve was obtained in a similar manner from the blood pool in the left ventricle. Dynamic ^{18}F-FDG analysis used a two tissue compartment model described by Phelps et al and Reivich et al and modified to incorporate decay of the radiotracer as previously described (14,20–22). From FDG compartmental analysis FDG transport [K_1, mL/min/g] and the FDG metabolism flux constant [Ki, mL/min/g] were selected as response measures for comparison to the DCE-MRI parameters (1,14).

PET and MRI images were evaluated independently by different researchers (PET: RD, LD; MRI: RV, SP), and those taking the PET measurements were blinded to DCE findings and vice versa. However both groups had access to the medical record describing the size and location of the primary breast lesion under investigation.

NIH-PA Author Manuscript

NIH-PA Author Manuscript

NIH-PA Author Manuscript

Pathological Assessment

Pathological response was determined from measurements and descriptions in surgical pathology reports at the time of surgery. Complete pathologic response (pCR) was defined as no recognizable invasive tumor cells remaining in the breast (ductal carcinoma in situ may be present).

Statistical Analysis

Percent changes with treatment were calculated for DCE-MRI and PET parameters. Spearman rank-order correlation coefficients, ρ, were calculated between changes in DCE-MRI parameters peak SER and peak PE with changes in PET parameters ^{18}F-FDG Ki and K_1 using SAS/STAT software, version 9.1 (SAS Institute, Cary, North Carolina) and R version 2.8.1 (R Foundation for Statistical Computing, Vienna, Austria). Responses in patients with and without complete pathologic response (pCR) were compared by Mann-Whitney U test, and exact p-values were calculated. All tests were two-tailed. As four combinations were evaluated for each statistical test (SER and PE by Ki and K_1), a Bonferroni adjustment for multiple comparisons recommended that P values < 0.05/4 = 0.0125 be considered statistically significant.

RESULTS

Fourteen patients undergoing neoadjuvant therapy for LABC met the inclusion criteria and were evaluated in the study. Patient characteristics are given in Table 1. Each patient underwent serial imaging by DCE-MRI and ^{18}F-FDG-PET at corresponding time points, performed between 0 and 27 days apart (mean, 7 days). Nine of the 14 patients were imaged pre- and mid- treatment (after at least 7 cycles of chemotherapy and prior to paclitaxel) and five were imaged pre-and post- treatment (following all chemotherapy and paclitaxel). Baseline tumor longest diameter (measured on DCE-MRI) ranged from 2.7 to 10.3 cm (median, 5.2 cm). One tumor was a grade 3 invasive lobular carcinoma, 11 were grade 3 invasive ductal carcinomas, and the remaining two were grade 1 and 2 invasive ductal carcinomas. Pathologic complete response was achieved in 5 (36%) cases, and 9 (64%) patients had residual disease ranging from microscopic foci to over 6 cm of invasive disease. All of the complete responders had grade 3 invasive ductal carcinomas.

Associations Between Changes in MRI and PET Tumor Measures

Figure 1 shows scatterplots of percent change in DCE-MRI and PET parameters. Regression fits and Spearman rank-order correlations illustrate the magnitude and strength of linear associations. Strong correlations were observed between changes in DCE-MRI SER and PET K_1 (ρ=0.83, $p<0.001$). Change in SER correlated moderately with change in PET Ki (ρ=0.71, p=0.004). MRI PE changes were also correlated with changes in both PET K_1 (ρ=0.61, p=0.019, noting that this was not considered statistically significant after Bonferroni correction) and Ki (ρ=0.76, p=0.002). Changes in PET Ki were significantly correlated with changes in MRI tumor volume (ρ=0.79, p=0.001), while changes in K_1 were not (ρ=0.51, p=0.064). Figure 2 illustrates a typical response with changes on DCE-MRI correlating closely with changes on PET. Alternatively, Figure 3 represents a case where changes in PET characteristics were more dramatic than DCE-MRI kinetics.

Differences Between Complete Responders and Others

Figure 4 compares percent change in MRI and PET parameters based on pathologic complete response (pCR) status. For all measures, percent change was greater on average for the 5 patients with pCR, compared to the 9 with residual disease. Two-sided Mann-Whitney U tests rejected the null hypothesis that the changes in MRI kinetic parameters (SER and

NIH-PA Author Manuscript

NIH-PA Author Manuscript

NIH-PA Author Manuscript

PE) were the same for those with pCR and residual disease ($p < 0.0125$), and suggested that changes in PET parameters differed by pCR as well ($p < 0.05$). Differences in the change in MRI functional tumor volume also showed a trend towards significance ($p = 0.06$). In particular (for this small sample), MRI PE values showed tightly clustered and distinct patterns of response. PE decreased at least 60% for all patients with pCR but less than 40% for all but one patient with residual disease.

DISCUSSION

This study measured associations between functional changes reflected by DCE-MRI and dynamic FDG-PET in breast tumors undergoing neoadjuvant chemotherapy. Both modalities demonstrated significant changes in the tumors with treatment, with greater changes observed in the patients who experienced complete pathologic response compared to those who still had residual disease at the time of surgery. To our knowledge, this is the first investigation to assess the association between treatment response markers by dynamic ^{18}F-FDG PET and DCE-MRI.

Our observation that mean changes in each measure (Ki, K_1, SER, PE, and volume) were smaller in patients with residual disease at completion of treatment compared to those with complete pathologic response agrees with prior findings of persistent blood flow (4), metabolism (2,5,6), and functional tumor volume (10) in tumors resistant to therapy. Treatment-induced changes in glucose delivery rate (PET K_1) were closely correlated with changes in tumor vascularity as reflected by DCE-MRI SER. This is not surprising as it was previously shown that both K_1 and SER correlate strongly with tumor blood flow, as measured by ^{15}O-Water PET (14,16). Also, changes in tumor metabolic activity (PET Ki) correlated closely with changes in functional tumor volume on MRI, an association that is expected for response to cytotoxic chemotherapy.

Although this study showed comparable changes in tumor perfusion and metabolism in response to cytotoxic chemotherapy, independent measurement of both characteristics may be particularly important for evaluating other targeted therapies where differences between effects on metabolism and perfusion may be informative for understanding mechanisms of tumor response and resistance. Furthermore, a multimodality approach using MRI and PET may optimize sensitivity for measuring response by providing detailed assessment of changes in tumor perfusion and extent by DCE-MRI along with early predictive changes in metabolism by ^{18}F-FDG-PET. This approach, as described by Specht et al, is currently being tested in a study to evaluate treatment effects of a targeted anti-vascular agent for treating breast cancer (23).

Our study has limitations. This was a pilot study with a small sample size (n=14), allowing only basic comparisons between the MRI and PET imaging parameters and between pathologic response groups. Also, the retrospective study design resulted in variability of the treatment timepoint for the second imaging session: nine patients were imaged midway through treatment, while the other five were imaged at the end of treatment. The clinical DCE-MRI breast protocol in this retrospective analysis was optimized for high spatial resolution and did not allow calculation of pharmacokinetic parameters. Instead, an established semi-quantitative analysis approach was used to differentiate low, medium, and high vascular density and permeability of the tumors (24,25). In this study we did not correct for potential bias due to partial volume effects in the serial PET measures. Shrinking tumor size could cause overestimation of the changes in PET measures (on the order of 10%) as previously described (4). However, partial volume correction techniques can introduce additional errors (14), and in this group of patients with relatively large LABC tumors ranging from 2.7 to 10.3 cm in diameter, the partial volume effects were likely minimal. It is

NIH-PA Author Manuscript

NIH-PA Author Manuscript

NIH-PA Author Manuscript

also important to note that MRI and PET images were not spatially registered due to differences in patient positioning (prone versus supine), and it was not possible to determine whether the hotspot-based PET and MRI ROI measurements came from the same areas within the tumors. Other investigators have utilized prone positioning devices for performing PET scans (15,26–29), which would greatly facilitate spatial registration of PET and MR images and will be explored in our future work. Furthermore, combined PET/MRI systems are currently in technical development and have the potential to not only provide coregistered images, but also substantially reduce the time and costs associated with obtaining data from both modalities. For this pilot study, the reproducibility of the PET and MRI measurement techniques was not assessed, although the reproducibility of the PET approach has been investigated previously (30).

In conclusion, changes in tumor size, metabolism and vascularity measured by ^{18}F-FDG-PET and DCE-MRI were well correlated and predictive of pathologic response in the setting of LABC treated with neoadjuvant chemotherapy. Further work is underway to explore the combined information from DCE-MRI and PET in assessing treatment response (23).

Acknowledgments

Grant Support:

Supported by National Institutes of Health Grants CA72064 and CA42045, NCI Cancer Center Support Grant (Comprehensive) - Biostatistics Shared Resource P30 CA015704, and Fred Hutchinson Cancer Research Center Cancer Center Support Grant Pilot Grant 015704

References

1. Dunnwald LK, Gralow JR, Ellis GK, et al. Tumor metabolism and blood flow changes by positron emission tomography: relation to survival in patients treated with neoadjuvant chemotherapy for locally advanced breast cancer. J Clin Oncol. 2008; 26:4449–4457. [PubMed: 18626006]
2. Kumar A, Kumar R, Seenu V, et al. The role of 18F-FDG PET/CT in evaluation of early response to neoadjuvant chemotherapy in patients with locally advanced breast cancer. Eur Radiol. 2009; 19:1347–1357. [PubMed: 19214522]
3. Mankoff DA, Dunnwald LK, Gralow JR, et al. Blood flow and metabolism in locally advanced breast cancer: relationship to response to therapy. J Nucl Med. 2002; 43:500–509. [PubMed: 11937594]
4. Mankoff DA, Dunnwald LK, Gralow JR, et al. Changes in blood flow and metabolism in locally advanced breast cancer treated with neoadjuvant chemotherapy. J Nucl Med. 2003; 44:1806–1814. [PubMed: 14602864]
5. McDermott GM, Welch A, Staff RT, et al. Monitoring primary breast cancer throughout chemotherapy using FDG-PET. Breast Cancer Res Treat. 2007; 102:75–84. [PubMed: 16897427]
6. Rousseau C, Devillers A, Sagan C, et al. Monitoring of early response to neoadjuvant chemotherapy in stage II and III breast cancer by [18F]fluorodeoxyglucose positron emission tomography. J Clin Oncol. 2006; 24:5366–5372. [PubMed: 17088570]
7. Ah-See ML, Makris A, Taylor NJ, et al. Early changes in functional dynamic magnetic resonance imaging predict for pathologic response to neoadjuvant chemotherapy in primary breast cancer. Clin Cancer Res. 2008; 14:6580–6589. [PubMed: 18927299]
8. Li KL, Partridge SC, Joe BN, et al. Invasive breast cancer: predicting disease recurrence by using high-spatial-resolution signal enhancement ratio imaging. Radiology. 2008; 248:79–87. [PubMed: 18566170]
9. Padhani AR, Hayes C, Assersohn L, et al. Prediction of clinicopathologic response of breast cancer to primary chemotherapy at contrast-enhanced MR imaging: initial clinical results. Radiology. 2006; 239:361–374. [PubMed: 16543585]

NIH-PA Author Manuscript

NIH-PA Author Manuscript

NIH-PA Author Manuscript

10. Partridge SC, Gibbs JE, Lu Y, et al. MRI measurements of breast tumor volume predict response to neoadjuvant chemotherapy and recurrence-free survival. AJR Am J Roentgenol. 2005; 184:1774–1781. [PubMed: 15908529]
11. Mankoff DA, Dunnwald LK, Partridge SC, Specht JM. Blood flow-metabolism mismatch: good for the tumor, bad for the patient. Clin Cancer Res. 2009; 15:5294–5296. [PubMed: 19706819]
12. Groves AM, Wishart GC, Shastry M, et al. Metabolic-flow relationships in primary breast cancer: feasibility of combined PET/dynamic contrast-enhanced CT. Eur J Nucl Med Mol Imaging. 2009; 36:416–421. [PubMed: 18818917]
13. Semple SI, Gilbert FJ, Redpath TW, et al. The relationship between vascular and metabolic characteristics of primary breast tumours. Eur Radiol. 2004; 14:2038–2045. [PubMed: 15316743]
14. Tseng J, Dunnwald LK, Schubert EK, et al. 18F-FDG kinetics in locally advanced breast cancer: correlation with tumor blood flow and changes in response to neoadjuvant chemotherapy. J Nucl Med. 2004; 45:1829–1837. [PubMed: 15534051]
15. Brix G, Henze M, Knopp MV, et al. Comparison of pharmacokinetic MRI and [18F] fluorodeoxyglucose PET in the diagnosis of breast cancer: initial experience. Eur Radiol. 2001; 11:2058–2070. [PubMed: 11702142]
16. Eby PR, Partridge SC, White SW, et al. Metabolic and vascular features of dynamic contrast-enhanced breast magnetic resonance imaging and (15)O-water positron emission tomography blood flow in breast cancer. Acad Radiol. 2008; 15:1246–1254. [PubMed: 18790395]
17. Chen X, Moore MO, Lehman CD, et al. Combined use of MRI and PET to monitor response and assess residual disease for locally advanced breast cancer treated with neoadjuvant chemotherapy. Acad Radiol. 2004; 11:1115–1124. [PubMed: 15530804]
18. Semple SI, Staff RT, Heys SD, et al. Baseline MRI delivery characteristics predict change in invasive ductal breast carcinoma PET metabolism as a result of primary chemotherapy administration. Ann Oncol. 2006; 17:1393–1398. [PubMed: 16788001]
19. Partridge SC, Heumann EJ, Hylton NM. Semi-automated analysis for MRI of breast tumors. Stud Health Technol Inform. 1999; 62:259–260. [PubMed: 10538368]
20. Phelps ME, Huang SC, Hoffman EJ, Selin C, Sokoloff L, Kuhl DE. Tomographic measurement of local cerebral glucose metabolic rate in humans with (F-18)2-fluoro-2-deoxy-D-glucose: validation of method. Ann Neurol. 1979; 6:371–388. [PubMed: 117743]
21. Reivich M, Alavi A, Wolf A, et al. Glucose metabolic rate kinetic model parameter determination in humans: the lumped constants and rate constants for [18F]fluorodeoxyglucose and [11C]deoxyglucose. J Cereb Blood Flow Metab. 1985; 5:179–192. [PubMed: 3988820]
22. Reivich M, Kuhl D, Wolf A, et al. The [18F]fluorodeoxyglucose method for the measurement of local cerebral glucose utilization in man. Circ Res. 1979; 44:127–137. [PubMed: 363301]
23. Specht, J.; Partridge, S.; Dunnwald, L., et al. DCE-MRI and dynamic FDG PET to monitor breast cancer response to neoadjuvant sunitinib in patients with locally-advanced breast cancer. Proceedings of the 31st Annual San Antonio Breast Cancer Symposium; San Antonio, TX. December 2008;
24. Li KL, Henry RG, Wilmes LJ, et al. Kinetic assessment of breast tumors using high spatial resolution signal enhancement ratio (SER) imaging. Magn Reson Med. 2007; 58:572–581. [PubMed: 17685424]
25. Esserman L, Hylton N, George T, Weidner N. Contrast-Enhanced Magnetic Resonance Imaging to Assess Tumor Histopathology and Angiogenesis in Breast Carcinoma. Breast J. 1999; 5:13–21. [PubMed: 11348250]
26. Goerres GW, Michel SC, Fehr MK, et al. Follow-up of women with breast cancer: comparison between MRI and FDG PET. Eur Radiol. 2003; 13:1635–1644. [PubMed: 12835979]
27. Imbriaco M, Caprio MG, Limite G, et al. Dual-time-point 18F-FDG PET/CT versus dynamic breast MRI of suspicious breast lesions. AJR Am J Roentgenol. 2008; 191:1323–1330. [PubMed: 18941064]
28. Moy L, Ponzo F, Noz ME, et al. Improving specificity of breast MRI using prone PET and fused MRI and PET 3D volume datasets. J Nucl Med. 2007; 48:528–537. [PubMed: 17401088]

NIH-PA Author Manuscript

NIH-PA Author Manuscript

NIH-PA Author Manuscript

29. Yutani K, Tatsumi M, Uehara T, Nishimura T. Effect of patients' being prone during FDG PET for the diagnosis of breast cancer. AJR Am J Roentgenol. 1999; 173:1337–1339. [PubMed: 10541114]

30. Minn H, Zasadny KR, Quint LE, Wahl RL. Lung cancer: reproducibility of quantitative measurements for evaluating 2-[F-18]-fluoro-2-deoxy-D-glucose uptake at PET. Radiology. 1995; 196:167–173. [PubMed: 7784562]

NIH-PA Author Manuscript
NIH-PA Author Manuscript
NIH-PA Author Manuscript

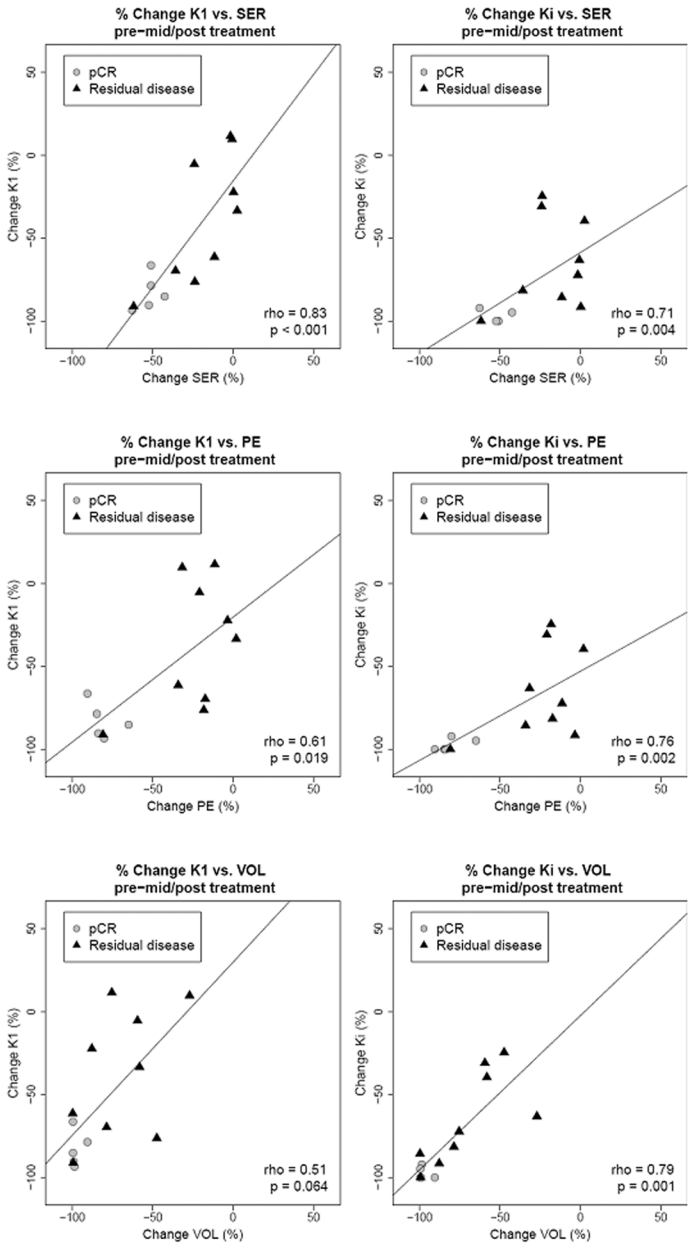

Figure 1.
Scatterplots of percent change from ^{18}F-FDG PET measures vs. percent change from DCE-MRI measures, with linear regression fit and Spearman rank-order correlation coefficient. Abbreviation: VOL = functional MRI tumor volume.

NIH-PA Author Manuscript

NIH-PA Author Manuscript

NIH-PA Author Manuscript

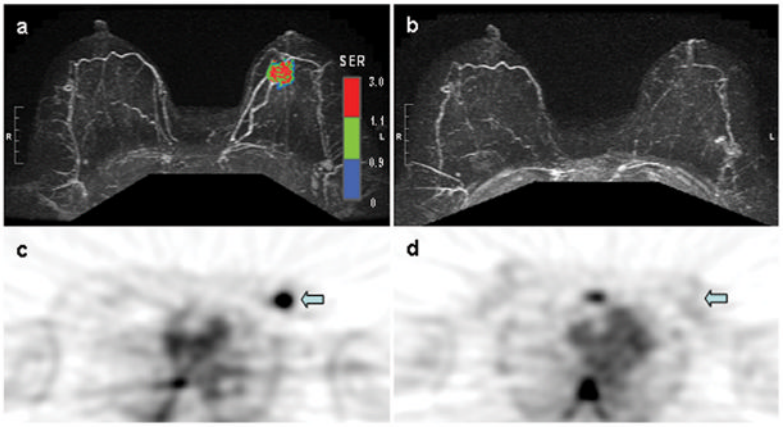

Figure 2.

Example of a patient who demonstrated similar levels of response in both PET and MRI parameters. This patient presented with a 2.7 cm high grade invasive ductal carcinoma, ER −/PR-/HER2−, and experienced a complete pathologic response to treatment. Shown are corresponding axial DCE-MRI and FDG-PET images before and during treatment. For this case, high percent changes in SER (−51%), PE (−85%), FDG K_1 (−78%), and FDG Ki (−100%) were observed at mid- treatment.

- **a.** DCE-MRI image with SER color overlay prior to chemotherapy.
- **b.** DCE-MRI image with SER color overlay at mid-treatment.
- **c.** FDG-PET image prior to chemotherapy, tumor indicated by arrow.
- **d.** FDG-PET image at mid-treatment, region of prior tumor indicated by arrow.

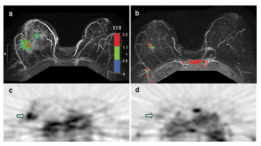

Figure 3.
Example of a patient who demonstrated different levels of response in the PET and MRI kinetic parameters. This patient presented with a high grade invasive ductal carcinoma extending over 10 cm through the breast, ER+/PR-/HER2+, and was found to have 3.5 cm of residual disease on pathology at the time of surgery. Shown are corresponding sagittal DCE-MRI and FDG-PET images before and during treatment. Like many patients in the study, this patient exhibited a dramatic reduction in tumor size. However, in this case the changes measured in PET parameters K_1 (−61%) and Ki (−86%) at mid-treatment were much larger than those observed in MRI kinetic parameters SER (−12%) and PE (−34%).

- **a.** DCE-MRI image with SER color overlay prior to chemotherapy.
- **b.** DCE-MRI image with SER color overlay at mid-treatment.
- **c.** FDG-PET image prior to chemotherapy, tumor indicated by arrow.
- **d.** FDG-PET image at mid-treatment, residual tumor indicated by arrow.

NIH-PA Author Manuscript NIH-PA Author Manuscript NIH-PA Author Manuscript

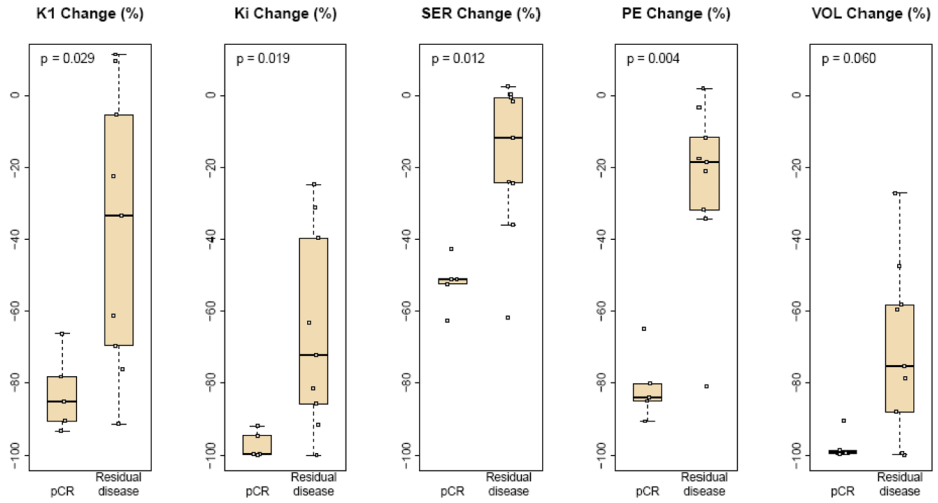

Figure 4.

Boxplots comparing percent changes from both ^{18}F-FDG PET and DCE-MRI measures by pathologic response status. P-values were computed using a Mann-Whitney U test to compare the measures between those who experienced pCR versus those with residual disease. Abbreviation: VOL = functional MRI tumor volume.

NIH-PA Author Manuscript
NIH-PA Author Manuscript
NIH-PA Author Manuscript

NIH-PA Author Manuscript

NIH-PA Author Manuscript

NIH-PA Author Manuscript

Table 1

Clinical and histologic characteristics for 14 patients in the study.

Characteristic	Median (Range) or n (%)
Age (years)	50 (35 – 65)
Initial tumor size (cm)*	5.2 (2.7 to 10.3)
Histologic Type:	
Invasive ductal	13 (93%)
Invasive lobular	1 (7%)
Tumor Grade[a]:	
1	1 (7%)
2	1 (7%)
3	12 (86%)
ER	
Positive	6 (43%)
Negative	8 (57%)
PR	
Positive	3 (21%)
Negative	11 (79%)
HER-2/*neu*	
Positive	4 (29%)
Negative	10 (71%)
Pathologic Response	
Complete	5 (36%)
Residual Disease	9 (64%)

Abbreviations: ER, estrogen receptor; PR, progesterone receptor

*Size measured for largest tumor diameter on DCE-MRI.

[a]Tumor grade was assessed prior to treatment

NIH-PA Author Manuscript

NIH-PA Author Manuscript

NIH-PA Author Manuscript

Table 2

Associations Between Changes in DCE-MRI and ^{18}F-FDG PET Parameters and Pathologic Response.

	Treatment Outcomes Residual Disease		
Tumor Measurements	**pCR mean (SD)**	**mean (SD)**	**p***
DCE-MRI			
Δ Volume (%)	−97 (4)	−70 (24)	0.060
Δ SER (%)	−52 (7)	−17 (21)	0.012
Δ PE (%)	−81 (10)	−24 (24)	0.004
^{18}F-FDG PET			
Δ K_1 (%)	−83 (11)	−38 (39)	0.029
Δ Ki (%)	−97 (4)	−65 (28)	0.019

*Exact p-values for differences between patients with pCR (n=5) and those with residual disease (n=9) evaluated by Mann-Whitney U test.

Abbreviations: Δ = change after chemotherapy, DCE-MRI=dynamic contrast-enhanced MRI, SER = signal enhancement ratio, PE = peak enhancement, PET = positron emission tomography, pCR = pathologic complete response